Reinvestigation of ^{56}Ni decay

Bhaskar Sur, Eric B. Norman, K. T. Lesko, Edgardo Browne, and Ruth-Mary Larimer
Nuclear Science Division, Lawrence Berkeley Laboratory, 1 Cyclotron Road, Berkeley, California 94720
(Received 12 February 1990)

In a series of experiments, we have reinvestigated the decay of the doubly magic nucleus ^{56}Ni, which is believed to be copiously produced in supernovae. We have confirmed its previously known decay scheme and half-life, and have searched for several rare decay modes. We establish an upper limit of 5.8×10^{-7} for the branching ratio of the second forbidden unique β^+ decay to the 158-keV level in ^{56}Co, leading to a lower limit of 2.9×10^4 yr for the half-life of fully ionized ^{56}Ni nuclei in cosmic rays. We also establish an upper limit of 5.0×10^{-3} for the branching ratio of the isospin forbidden Fermi electron capture transition to the 1451-keV level in ^{56}Co, which in turn leads to an upper limit of 124 keV for the isospin mixing Coulomb matrix element of the ^{56}Ni ground state.

I. INTRODUCTION

The doubly magic nucleus ^{56}Ni decays via an allowed electron capture (EC) transition to the 1720-keV level in ^{56}Co with an approximate 100% branch and a half-life of 6.0 days.[1] Although the decay of ^{56}Ni has been previously studied, we have reexamined its decay scheme specifically to search for two interesting but rare decay modes. The first mode is β^+ decay, which would be the dominant channel for the decay of fully ionized ^{56}Ni nuclei as relativistic cosmic rays. The second mode is the isospin forbidden electron capture transition to the 1451-keV level in ^{56}Co, which if found, could be used to calculate the isospin mixing in the ground state of ^{56}Ni. In the course of these experiments, we have also reconfirmed the coincidence relationships, γ-ray branches, and half-life for the decay of ^{56}Ni in the laboratory.

The $N=Z=28$ nuclide ^{56}Ni is the most abundantly produced isotope in the silicon burning stage of a ≥ 10 solar-mass star. After this stage, the energy available from fusion of light nuclei is exhausted, and the star undergoes gravitational collapse resulting in a shock wave and supernova explosion. The light output from the supernova remnant is largely due to the energy from the radioactive decay of the ^{56}Ni and its daughter ^{56}Co ($t_{1/2}=77.08\pm0.08$ days[2]). This prediction has been corroborated by the observation[3] of the 77.1 day exponential decay of the light output from supernova 1987A. It has been hypothesized that supernovae are sites for acceleration of relativistic nuclei found in cosmic rays. If that is so, ^{56}Ni is one of the species that will almost certainly be accelerated and stripped of its atomic electrons. The bare ^{56}Ni nucleus in cosmic rays is thus unable to decay via electron capture, but as shown in Fig. 1, it is energetically possible for it to β^+ decay to the 0-, 158-, and 970-keV levels in ^{56}Co with $J^\pi=4^+$, 3^+, and 2^+, respectively. Since decay to the ground state takes place through a fourth forbidden transition, and decay to the 970-keV level has only 144 keV of available energy, it has been suggested that the second forbidden unique transition to the 158-keV level is the most likely of these possibilities.[4] From studies of the decays of ^{10}Be, ^{22}Na, and ^{26}Al, the logft values for such transitions have been found[4,5] to be between 13.9 and 15.7, yielding an estimate of 8.5×10^4 yr $< t_{1/2} < 5.4\times10^6$ yr for the β^+ partial half-life of ^{56}Ni. Because of this long lifetime after it has been stripped of its electrons, ^{56}Ni would survive in the cosmic rays. Depending on the value of this β^+ decay half-life, future measurements of its abundance in the cosmic rays could be used to determine the time interval between production and acceleration, or the cosmic-ray confinement time in the galaxy.[6] We searched for the positron decay branch of ^{56}Ni in the laboratory by attempting to measure the energy spectrum of emitted positrons in coincidence with deexcitation γ rays from the resulting ^{56}Co nucleus and the back-to-back 511-keV photons from positron annihilation.

The other rare decay mode for which we have specifically searched is the electron capture decay of ^{56}Ni to the 1451-keV level in ^{56}Co. This $0^+\rightarrow0^+$ Fermi transition is forbidden because the initial and final states have different isospins. However, such transitions are known to occur because of the isospin impurities induced by the Coulomb interaction in the nuclear states. The previously observed isospin forbidden transitions and the resulting isospin impurities have been reviewed by Raman, Walkiewicz, and Behrens.[7] We employed two experimental techniques to look for this decay mode of ^{56}Ni. The first technique involved an accurate determination of the γ-ray feedings into and out of the 1451-keV level by measuring the relative intensities of these γ rays with a well calibrated intrinsic germanium spectrometer. Any excess intensity out of this level would be due to the direct electron capture population of this level. This experiment yielded a result consistent with no direct EC feeding and allowed us to set an upper limit on the branching ratio for the transition. The second technique consisted of a determination of the direct population of this level by observing the sum deexcitation energy of 1451 keV in a germanium detector in anticoincidence with the 269-keV γ-ray feeding the level. The 269-keV γ rays were detected in an annular NaI detector surround-

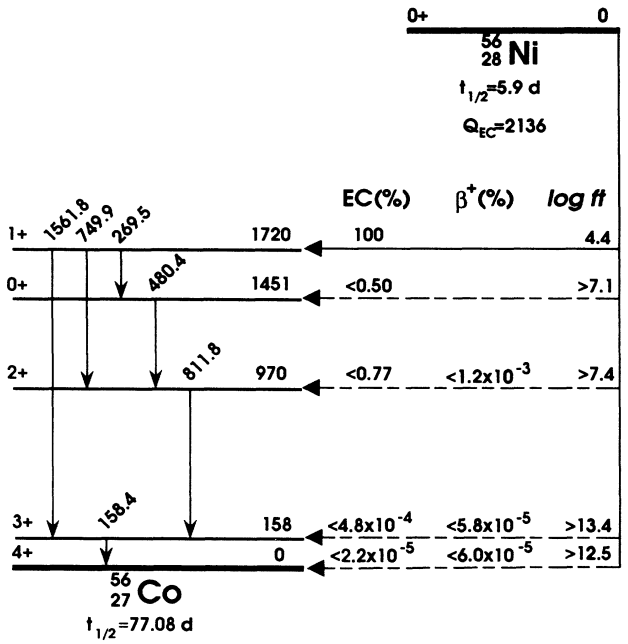

FIG. 1. Decay scheme for ^{56}Ni showing EC and β^+ branching ratios measured in this work.

ing the source. The ratio of this event rate to that measured in singles is directly related to the branching ratio for the isospin forbidden Fermi transition. This experiment also yielded a branching ratio consistent with zero.

II. β^+ DECAY SEARCH

A. Source preparation

The ^{56}Ni was produced via the ^{56}Fe(^{3}He,$3n$) reaction at the Lawrence Berkeley Laboratory's 88-Inch Cyclotron. For each production run, a stack of approximately 7 natural iron foils, each 20 mg/cm^2 thick were irradiated with a $\approx$5-μA beam of 50-MeV ^{3}He ions for about 8 h. The irradiated foils were allowed to "cool" for approximately one week allowing the short lived activities to decay away, as well as reducing the activity of the simultaneously produced ^{57}Ni. The beam spots on the target foils were then carefully cut out and dissolved in concentrated HCl plus a few drops of HNO_3. This solution was then passed through an AG 1-X8 anion exchange resin column to remove the cobalt and iron fractions. The nickel fraction was subsequently precipitated as nickel dimethylglyoxime (Ni-DMG), and the red Ni-DMG precipitate was deposited on a 0.025-mm-thick polyethylene backing, evaporated to dryness, and covered with a second polyethylene layer. This procedure sealed the activity while allowing electrons and positrons to escape from the source with a minimum of energy loss. The residual ^{57}Ni proved to be invaluable as in *in-situ* source for efficiency calibrations in the β^+ decay search. For the γ-ray counting experiments, the sources prepared in this fashion were further covered with two layers of plastic tape in order to ensure that the low-energy ($\approx$6.9 keV) x rays, coincident with the γ rays from EC decay, did not escape from the source.

B. Experimental arrangement for detecting β^+ transitions

The configuration of detectors used to search for the β^+ decay of ^{56}Ni to the 158- and 970-keV levels in ^{56}Co is shown schematically in Fig. 2. The source of ^{56,57}Ni was mounted at the center of the 9.2-cm-diameter cylindrical cavity of a 30-cm$\times$30-cm NaI annular detector which was optically divided into two halves. Two 1000-μm-thick silicon surface barrier detectors were placed immediately on either side of the source to detect the emitted positrons. Two 110-cm^3 high-purity germanium (Ge) detectors were placed behind the silicon detectors, but still within the NaI annulus. Test runs with ^{57}Ni and ^{22}Na sources showed that the most efficient and lowest background mode for operating this detector ensemble was to detect the 511-keV photons from positron annihilation in both halves of the NaI annular detector and the coincident γ ray in one of the Ge detectors.

Consequently, the electronic event trigger circuitry required coincident signals between at least one silicon detector, at least one Ge detector, and both halves of the NaI detector. For each such trigger, the energy signals from all six detectors (two Si, two Ge, and both halves of the annular NaI detector) were recorded on magnetic tape for subsequent off-line analysis. No attempt was made to record the time relationships between any of the coincident detector signals, because it was found that the four-fold hardware trigger eliminated practically all random coincidences. The trigger rate was approximately 300 Hz. The activities of ^{56}Ni and ^{57}Ni in the source were determined by measuring the intensities of known γ rays with an efficiency-calibrated germanium detector system. Since there was significant energy loss for low-energy electrons and positrons in the ^{56,57}Ni source, the energy calibration for the silicon detectors was done with conversion electron lines from ^{56}Ni *in situ*. The total efficiency for detecting positrons was determined using

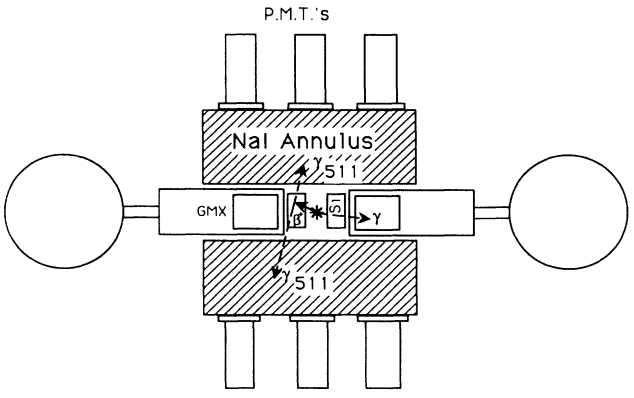

FIG. 2. Experimental arrangement for β^+ decay search.

positrons in coincidence with 1377-keV γ rays from the ^{57}Ni activity also contained in the source. Finally, the relative photopeak efficiencies of the Ge detectors were obtained by using standard γ-ray sources of ^{57}Co, ^{203}Hg, ^{137}Cs, ^{60}Co, and ^{22}Na mounted at the source position. The β^+ signal from the sought-after decay to the 970-keV level was found to be contaminated by residual interactions of the γ rays and conversion electrons from the ^{56}Ni activity. This was caused by the thickness of the source, the low end-point energy of the expected β^+ spectrum, and the poor energy resolution of the NaI detectors. Hence, we were unable to observe this direct β^+ transition. However, we infer a limit on this decay branch from the γ-intensity balance experiment using a theoretical EC/β^+ ratio.

Because the hardware trigger in the above setup required that at least three photons (the 511-511-keV annihilation radiation as well as the nuclear γ rays) be detected in the Ge and NaI detectors, it could not be used in the search for β^+ transitions of ^{56}Ni to the ground state of ^{56}Co. The data for the analysis of these transitions were taken with an additional version of the experiment using only one silicon detector where the hardware trigger required any three of the total of five detectors (one Si, two Ge, and both halves of the annular NaI detector) to have had coincident signals. This experiment was carried out with a thinner and weaker ^{56,57}Ni source. In later off-line analysis, the ground-state to ground-state β^+ transition from ^{56}Ni was searched for by sorting out those events where a β^+ was detected in the Si detector along with just the annihilation 511-keV photons in both halves of the NaI detector, and by requiring no signal from the Ge detectors.

C. Analysis of β^+ transitions

The six parameter event-by-event data (β^+ transitions in coincidence with nuclear γ rays) and the five parameter data (β^+ transitions to the ground state) were both sorted off-line with a variety of software gates. The candidate positron spectra for β^+ decay to the excited states in ^{56}Co were extracted by projecting out the energy spectrum of each of the silicon detectors in coincidence with a 158-keV γ ray in one of the Ge detectors and the annihilation 511-keV photons in both halves of the NaI annulus. Si background spectra were extracted by placing gates above and below the Ge γ-ray photopeaks. As mentioned previously, the efficiency of this arrangement for detecting the coincident β^+-γ was determined *in situ* using the same gating procedure on the known β^+ decay of ^{57}Ni to the 1377-keV level in ^{57}Co. This efficiency was scaled for the various ^{56}Ni γ-ray energies.

The gated, background-subtracted energy spectrum in one of the silicon detectors due to positronlike events from decay to the 158-keV level is shown in Fig. 3(a). The large number of events in the low-energy region of the spectrum is due to the EC decay of ^{56}Ni which produces 1720 keV of electromagnetic energy. Because of the gating requirement of 1180 keV (=158+511+511) in the Ge and NaI detectors, the β^+ spectra in the Si detector were contaminated with events with energies up to 540 keV (1720–1180) due to Compton scattered γ rays and conversion electrons. Due to the relatively poor energy resolution of the NaI detectors ($\approx$50 keV wide gates for 511-keV photons), these events actually extend out to 635 keV in the Si spectrum. Thus the region of the spectrum sensitive to β^+ events extends from 635 keV to the end-point energy of 956 keV, i.e., the upper 33.5% region of the β^+ spectrum. The efficiency for detecting positrons was therefore deduced using the upper 33.5% region of the positron spectrum from the decay of ^{57}Ni in coincidence with 1377-keV γ rays, shown in Fig. 3(b). The total efficiency of this arrangement for detecting positron decay to the 158-keV level was found to be 4.8×10^{-3}. In a running time of about 6 days with a 1.2 μCi source, the number of candidate events was 18$\pm$14.5. Conservatively, this corresponds to an upper limit of 26 events (68% confidence level) and a branching ratio of $\leq 5.8\times10^{-7}$.

The five-parameter data were also sorted off-line for β^+ decay to the ground state, and the candidate positron spectrum was extracted by requiring an energy signal in the Si detector with coincidence gates set at 511 keV in both NaI detectors, and anticoincidence gates set also on

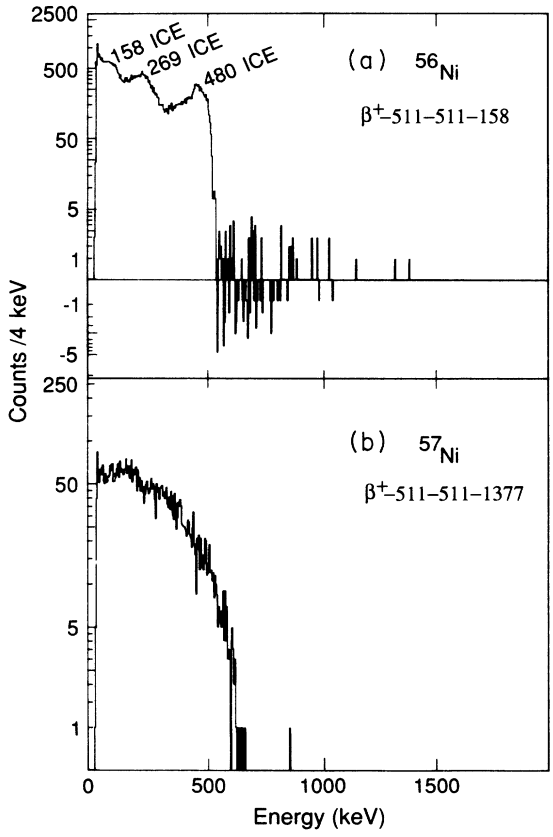

FIG. 3. Gated, background-subtracted spectra derived from β^+ decay search data: (a) candidate positron spectrum in coincidence with 158-keV γ rays from ^{56}Ni; (b) spectrum of positrons in coincidence with 1377-keV γ rays from ^{57}Ni.

both Ge detectors. Background energy spectra of the Si detector were obtained by requiring Si events in coincidence with combinations of gates above and below 511 keV in each of the NaI detectors. The lower energy part of the candidate positron spectrum was again found to be contaminated, by positrons with energies up to 866 keV from the decay of ^{57}Ni, where the coincident 1377-keV (and sometimes 127-keV) γ ray had escaped detection. The sensitive energy region was from 874 keV to the end-point energy of 1114 keV, i.e., the upper 21.5% region of the β^+ spectrum. The efficiency for this mode of detecting positrons was also deduced from the decay of *in situ* ^{57}Ni, and also by using a separate ^{22}Na source. The efficiency for detecting the ground-state to ground-state positron transition is

$$\epsilon_{\beta\text{-}511\text{-}511}=(\epsilon_{\beta\text{-}511\text{-}511\text{-}\gamma})/(\epsilon_\gamma)\ , \tag{2.1}$$

where $\epsilon_{\beta\text{-}511\text{-}511\text{-}\gamma}$ is the measured efficiency for coincident β^+ and γ from the decay of ^{57}Ni and ^{22}Na. ϵ_γ is the measured photopeak efficiency of the Ge detector for detecting the 1377-keV or the 1275-keV γ rays. The corresponding efficiency for detecting positron emission in the upper 21.5% region of the spectrum was found to be 1.56×10^{-3}.

The background subtracted positron spectrum showed a few events recorded in the sensitive energy interval (874–1114 keV). However, the number of these events increased as the experiment progressed. These were apparently caused by positrons from the decay of ^{56}Co growing in the ^{56}Ni source. The candidate counts, which were binned into $\approx$1 day intervals, were found to be consistent with a composite curve that included the 6 day growth and 77.1 day decay of the ^{56}Co component. The initial β^+ count rate from ^{56}Ni was $(-0.6\pm2.2)\times10^{-5}$ counts/s; a result which is consistent with no β^+ transition to the ground state. The initial activity of ^{56}Ni used in this experiment was 0.55 μCi, which results in an upper limit of 6.0×10^{-7} (68% confidence level) for the β^+ branching ratio of ^{56}Ni to the ground state of ^{56}Co.

III. γ-RAY INTENSITIES

Absolute EC decay branchings to excited levels in ^{56}Co can be deduced from γ-ray intensity balances. The small expected branchings to the levels below 1720 keV, however, require that the γ-ray intensities be very precisely measured. Existing experimental intensities[8–10] have fractional uncertainties $\geq$4%, which are not sufficiently precise for determining the decay branchings. The normalization of relative γ-ray intensities to absolute values assumes no electron capture population to levels below the 970-keV level, and uses the combined intensity for the 811- and 1562-keV transitions as the total disintegration intensity of ^{56}Ni. These transitions provide the most precise value for that quantity.

A. Experimental arrangement

The relative γ-ray intensities in the electron capture decay of ^{56}Ni were determined from a spectrum measured with a 110-cm^3 high-purity Ge coaxial detector. The ^{56}Ni source was placed 23 cm from the detector to reduce true coincidence summing effects. The data were stored on magnetic disk and later analyzed with the code SAMPO.[11] The fractional uncertainties were approximately equal to 1% in the detector relative photopeak efficiencies for the various γ-ray energies, and $\leq$1% in the individual photopeak areas. With each contributing about equally to the precision of the measured intensities, careful attention was given to the determination of both.

B. Analysis of γ-ray intensity balance experiment

Known γ rays from the decays of ^{133}Ba and ^{152}Eu were used to determine the detector photopeak efficiencies by placing separately a $\approx$1 μCi ^{133}Ba and a $\approx$10 μCi ^{152}Eu source in the same geometry as that of the ^{56}Ni source. The γ-ray intensity values were taken from Chauvenet[12] for ^{133}Ba, and from Debertin,[13] and Yoshizawa *et al.*[14] for ^{152}Eu. Fractional uncertainties of $<$1% reported by these authors include both statistical components and those in the detector efficiencies.

Corrections to the photopeak areas due to true coincidence summing were calculated for ^{133}Ba, as described by Debertin and Helmer[15] with the computer code KORSUM,[16] and using γ-ray data and decay schemes from Ref. 1. The effect of summing with x rays was included in the calculation. The total efficiencies were determined with calibrated sources of ^{57}Co, ^{203}Hg, ^{22}Na, and ^{137}Cs (122–661-keV range), and from the data of Helmer[17] (higher energies) for a 114-cm^3 Ge detector with the source placed 20 cm away. The correction factors were $\leq$1.007 for γ rays with energies between 200 and 1528 keV. The resulting relative photopeak efficiencies are given in Table I.

Photopeak efficiencies for specific γ-ray energies can be interpolated between the calibration values listed in Table I. Debertin and Helmer[15] recommend the following fitting function between 200 and 2000 keV:

$$\epsilon=c\left[\frac{E}{E_0}\right]^{-a_1}\ , \tag{3.1}$$

TABLE I. Relative photopeak efficiencies for 110-cm^3 high-purity Ge detector for ^{133}Ba and ^{152}Eu sources placed 23 cm from detector.

E_γ (keV)	Relative ϵ	E_γ (keV)	Relative ϵ
81.0	8.638±0.143	586.3	2.226±0.032
121.8	8.100±0.072	688.6	1.867±0.025
160.6	6.953±0.287	778.9	1.746±0.011
223.2	5.789±0.072	810.4	1.720±0.032
244.6	5.161±0.047	867.4	1.588±0.007
295.9	4.301±0.065	919.4	1.513±0.029
302.8	4.197±0.018	964.1	1.448±0.007
344.2	3.710±0.025	1085.9	1.319±0.007
356.0	3.591±0.014	1112.1	1.298±0.007
367.8	3.444±0.029	1212.9	1.219±0.011
383.9	3.315±0.039	1299.1	1.133±0.007
411.1	3.161±0.018	1408.0	1.050±0.007
443.9	2.903±0.014	1528.1	1.000±0.023
488.7	2.606±0.032		

where E is the γ-ray energy, and c and a_1 are adjustable parameters that may be obtained from a least-squares fit analysis of the linearized equation:

$$\log_{10}\epsilon = \log_{10}c - a_1(\log_{10}E - \log_{10}E_0) . \quad (3.2)$$

A log-log plot of photopeak efficiency versus γ-ray energy shows a significant change of slope at about 700 keV. Hence, the efficiencies for γ rays with energies between 223 and 689 keV were fitted separately from those for higher energies. The results of these fits (for which $\chi\nu^2 = 1.0$) are displayed in Fig. 4, where ϵ/ϵ_0 is plotted as a function of the γ-ray energy. ϵ is the measured photopeak efficiency and ϵ_0 is its fitted value.

A typical γ-ray spectrum is shown in Fig. 5. The γ-ray energies and relative intensities for all the observed lines from ^{56}Ni are given in Table II. The fractional uncertainties of the detector efficiencies deduced from the fit are generally $\approx 0.5\%$. However a minimum value of 1% was used to account for possible correlations between the experimental uncertainties in the calibration standards. This value represents a typical experimental uncertainty of the calibration standards between ≈ 250 and ≈ 800 keV. Consequently, the relative intensities have fractional uncertainties of $\approx 1\%$, except for that of the 1562-keV γ ray, which has 4% uncertainty. This higher value is due to the extrapolated (from 1528 keV) and less precise photopeak efficiency. The relative intensity of the 158-keV γ ray was deduced from the intensity balance at the 158-keV level, using a conversion coefficient of 0.012 ± 0.001.[18] This value is more reliable than the directly measured intensity of 100 ± 4, which was determined using the less precise photopeak efficiency. Except for the 812- and 1562-keV γ rays, the relative intensities presented in this paper are more precise than and in fair agreement with those values evaluated by Junde *et al.*,[19] also shown in Table II.

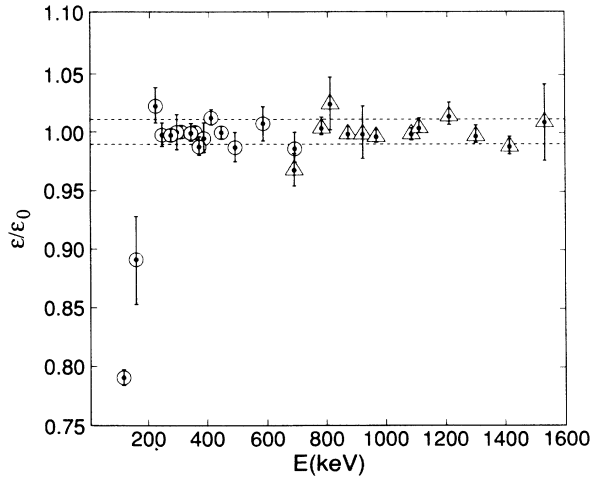

FIG. 4. Ratio of measured-to-fitted relative Ge photopeak efficiencies. The horizontal lines show the 1% error limits on the global fit. The fitted parameters in Eq. (3.1) are $c = 0.0970 \pm 0.0002$ and $a_1 = 0.974 \pm 0.009$ for $E \leq 688.7$ keV, and $c = 0.0385 \pm 0.0001$ and $a_1 = 0.833 \pm 0.012$ for $E \geq 688.7$ keV.

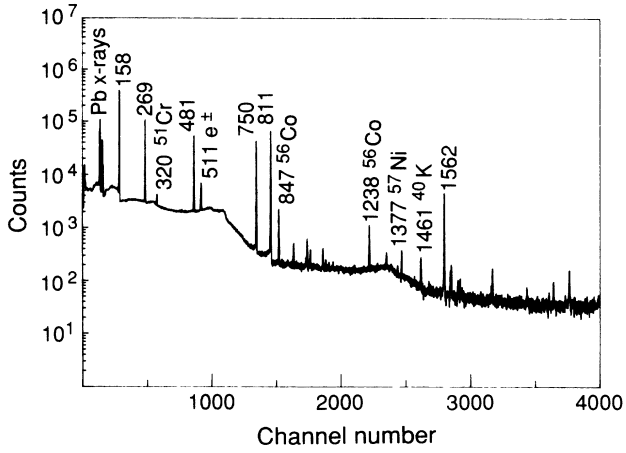

FIG. 5. γ-ray singles spectrum of ^{56}Ni taken for approximately 1 day with the source at a distance of 23 cm from a 110-cm^3 high-purity Ge detector. Peaks labeled only by energy are from ^{56}Ni.

Table III shows absolute decay branchings and corresponding logft values in ^{56}Ni decay to levels of ^{56}Co. These branchings were deduced from transition intensity balances using both γ-ray data from Ref. 19 and from this work. A decay branching of $<0.024\%$ to the 970-keV level, presented in a decay scheme in Ref. 18, is inconsistent with its corresponding γ-ray data. The transition intensities of the 269- and 480-keV γ rays were corrected for internal conversion, with experimental conversion coefficients of 0.0034 ± 0.0002 (Ref. 18) and $0.001\,50 \pm 0.000\,15$ (Ref. 18), respectively. The negative branchings deduced for the 970- and 1451-keV levels lead to upper limits for these quantities, which can be estimated as recommended by Lyons,[20] and by the Particle Data Group.[21]

C. The half-life of ^{56}Ni

The decay rate of the 269- and 480-keV γ rays from ^{56}Ni decay, normalized to that of the 320-keV γ ray from ^{51}Cr (source impurity) decay, was measured in 8 h periods

TABLE II. Relative γ-ray intensities from ^{56}Ni decay.

E_γ (keV)	I_γ (relative) Ref. 19	This work
158.4	100±1	100±1[a]
269.5	36.9±0.8	38.70±0.39
480.4	36.9±0.8	38.64±0.39
749.9	50.1±1.2	50.58±0.50
811.8	87.0±0.9	88.40±0.90
1561.8	14.2±0.6	12.77±0.41

[a] From intensity balance at the 158.4-keV level.

TABLE III. Absolute direct decay branching from γ-ray intensity balance in ^{56}Ni decay.

	Decay branching (%)					
	Measured value		Upper limit (68% C.L.)		logft	
E_x (keV)	Ref. 19	This work	Ref. 19	This work	Ref. 19	This work
0.0	0.0[a]	0.0[a]				
158	0.0[a]	0.0[a]				
970	−0.06±1.7	−0.86±1.10	1.7	0.77	≥7.1	≥7.4
1451	−0.07±1.1	−0.13±0.55	1.1	0.50	≥6.8	≥7.1
1720	100.0[b]	101.0±0.8			4.4	4.4

[a] Value assumed for a highly forbidden transition.
[b] Value assumed for decay-scheme normalization.

with a high-purity Ge detector for 5.5 consecutive days. The time for each measurement was determined by the internal clock on the data-acquisition IBM/PC computer. The clock's nominal accuracy was better than 26 s per month. By using the ratio of intensities of ^{56}Ni γ rays to that of ^{51}Cr, one reduces the effect of systematic uncertainties due to electronic dead time and also to possible accidental changes in the source-detector geometry.

A least-squares fit to the decay rate data of the experimental γ-ray intensity ratio gives 7.49±0.12 d for the quantity

$$\left[\frac{1}{T_{\mathrm{Ni}}}-\frac{1}{T_{\mathrm{Cr}}}\right]^{-1},$$

where T_{Cr} and T_{Ni} are the half-lives of ^{51}Cr and ^{56}Ni, respectively. Using $T_{\mathrm{Cr}}=27.702\pm0.002$ d,[22] one obtains $T_{\mathrm{Ni}}=5.9\pm0.1$ d. The major contribution to the uncertainty comes from the 1% statistical uncertainty in the intensity of the weak (compared to the 269- and 480-keV γ rays) ^{51}Cr 320-keV line contained in the γ-ray spectrum.

The experimental half-life deduced here is consistent with previous results of 6.0±0.5 d (Ref. 23) and 5.8±0.6 d,[24] but it disagrees with 6.4±0.1 d,[25] and with the very precise value of 6.10±0.02 d.[26] The reason for such disagreements could not be determined. The half-life given in Ref. 25 was deduced through a complex experimental procedure of growth and decay curves of ^{56}Ni and ^{56}Co, and the value presented in Ref. 26, from the decay rate of the 158- and 269-keV γ rays, measured "in a fixed geometry"[26] for 17 days. This latter measurement, however, was not described with enough detail, and the quoted uncertainty is probably statistical only.

IV. MEASUREMENT OF ISOSPIN FORBIDDEN BRANCHING RATIO USING 4π ANTICOINCIDENCE

A. Detector configuration

The detector configuration used to measure the EC branching ratio to the 1451-keV level in anticoincidence with 269-keV γ rays is shown in Fig. 6. The 1451-keV level in ^{56}Co decays by emission of a cascade of three γ rays as shown in Fig. 1. The corresponding 1451-keV triple γ-ray sum peak was detected with a single 110-cm^3 Ge detector placed as close to the source as possible. A plastic cap over the front face of the Ge detector prevented x rays and conversion electrons from being detected. In this configuration, the Ge detector was sensitive to photons emitted into an almost 2π steradian solid angle from the source, eliminating effects due to γ-ray angular correlations. The source and front face of the Ge detector were positioned in the center of the annular 30-cm×30-cm NaI detector and the remainder of the space was filled with a 7.5-cm×15-cm cylindrical NaI detector. A logic signal derived from the NaI detectors (with the energy threshold set just above their noise level) was used as an anticoincidence gate for the analog signals from the Ge detector. Both gated and ungated Ge signals were recorded on magnetic disc.

B. Analysis

Direct EC decay of the 0^+ ^{56}Ni ground state to the 0^+ 1451-keV state in ^{56}Co is forbidden by isospin conservation. This experiment was very sensitive to the direct EC feeding to the 1451-keV level, because of the almost 100% efficiency of the NaI detectors for the 269-keV γ

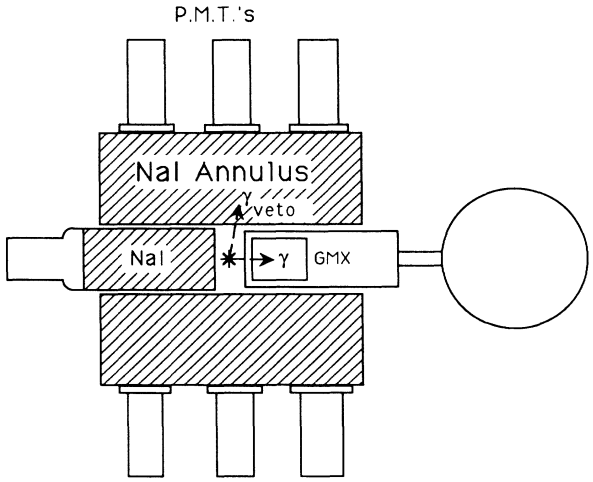

FIG. 6. Experimental arrangement for 4π anticoincidence experiment to measure isospin forbidden EC branching ratio to the 1451-keV level.

ray which feeds this level. The intensity of the 1451-keV γ-ray sum peak was measured with the Ge detector in anticoincidence with the NaI detector (N_v) and also in singles (N_s). One can derive expressions for these two count rates, using the efficiency for detecting the triple γ-ray sum peak at 1451 keV in the absence of any other radiation, $\Pi_\epsilon=\epsilon(480)\cdot\epsilon(811)\cdot\epsilon(158)$, i.e., the product of the individual photopeak efficiencies for the single γ-ray components of the sum peak. The singles counting rate is

$$N_s(1451)=S_0\Pi_\epsilon B_{269}\left[1-\frac{\epsilon_{T^{269}}}{1+\alpha}+\frac{B_{\rm IF}}{B_{269}}\right], \quad (4.1)$$

where S_0 is the disintegration rate of the source, B_{269}, the total (photon plus electron) emission probability of the 269-keV transition, $B_{\rm IF}$ is the isospin forbidden direct EC branching ratio, $\epsilon_{T^{269}}$ is the total Ge detection efficiency at 269 keV, and α is the total conversion coefficient of the same transition. The anticoincidence counting rate is given by

$$N_v(1451)=S_0\Pi_\epsilon B_{269}\left[1-\frac{\epsilon_{T^{269}}+T_{269}-P_{269}}{1+\alpha}+\frac{B_{\rm IF}}{B_{269}}\right], \quad (4.2)$$

where T_{269} is the total NaI detection efficiency for 269-keV photons and P_{269} is the probability for Compton scattering of a 269-keV photon between the NaI and the Ge detectors. From these equations, one deduces the following expression for the EC branching ratio:

$$B_{\rm IF}=\frac{B_{269}}{1+\alpha}\left[\frac{T_{269}-P_{269}}{1-[N_v(1451)/N_s(1451)]}-(1-\epsilon_{T^{269}}+\alpha)\right], \quad (4.3)$$

where the crucial experimentally determined quantities are $T_{269}-P_{269}$ and $[N_v(1451)/N_s(1451)]$, because they establish the precision of the measurement.

The quantity $T-P$, measured with other sum peaks, is a slowly varying function of γ-ray energy. $T-P$ values for 158 keV (0.76±0.01), 481 keV (0.78±0.02), and 811 keV (0.81±0.01) were determined using ^{56}Ni. Interpolating between these measured values leads to an estimate of $T_{269}-P_{269}=0.77\pm0.01$. The ratio $[N_v(1451)/N_s(1451)]$ was deduced from the Ge spectral areas under this sum peak measured in singles and in anticoincidence for several pairs of runs. The γ-ray spectra for a typical run are shown in Fig. 7. In order to ensure that the measured counting rates were not affected by varying dead times, efficiences, decay of ^{56}Ni, or by other spurious effects, the peak areas were normalized to the area under the 1720-keV sum peak. This peak, due to the sum of all the electromagnetic energy in the normal γ-ray cascade, cannot be vetoed—hence it is acquired at a constant rate per ^{56}Ni decay irrespective of the NaI anticoincidence. The measured ratio was

$$\frac{N_v(1451)}{N_s(1451)}=0.032\pm0.002\ .$$

The total Ge efficiency, measured at an energy of 279 keV using a calibrated ^{203}Hg source, gave $\epsilon_{T^{279}}=0.21\pm0.01$. Using these values and Eq. (4.3), one obtains $B_{\rm IF}\leq 6.1\times10^{-3}$ (68% C.L.).

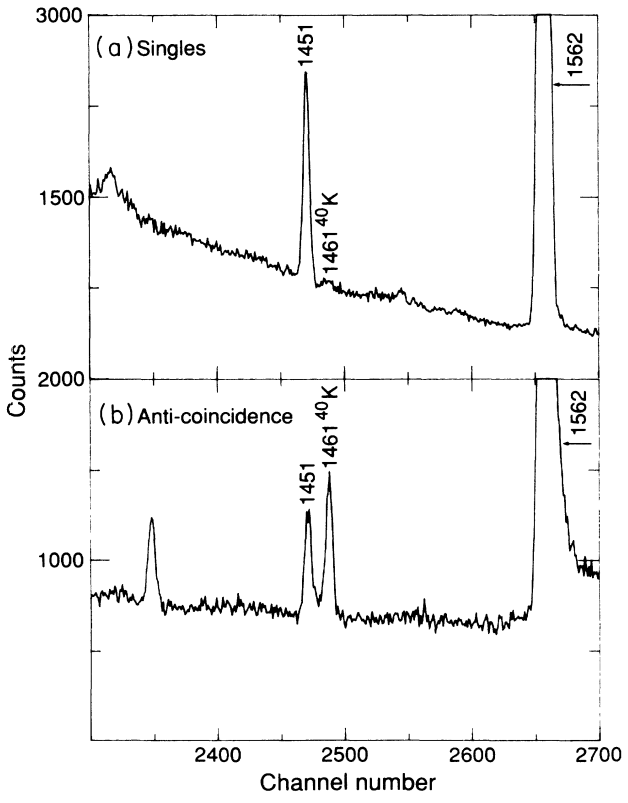

FIG. 7. Representative Ge spectra of the 1451-keV region from the 4π anticoincidence experiment: (a) singles mode (i.e., without NaI anticoincidence); and (b) with NaI anticoincidence.

V. CONCLUSIONS

Our "best" values for the direct EC and β^+ transitions to levels in ^{56}Co populated in the decay of ^{56}Ni are presented in Fig. 1. These 68% confidence-level upper limits[21] for the ground and first three excited states were deduced as follows.

(i) The β^+ branching ratio to the ground state was directly measured to be $\leq 6.0\times10^{-7}$. Since this is a fourth-forbidden non-unique transition, the EC/β^+ ratio and logft values were calculated as for an allowed transition. These values produced an upper limit of 2.2×10^{-7} for the EC branching ratio, and a lower limit of 12.5 for the logft value of this transition.

(ii) The β^+ branching ratio to the 158-keV level was experimentally determined to be $\leq 5.8\times10^{-7}$, and the corresponding limit of 4.8×10^{-6} for the EC decay was again deduced from the theoretical EC/β^+ ratio of 8.30 for a second-forbidden unique transition. The logft value was calculated to be ≥ 13.4.

(iii) The best value for the direct EC branching ratio to the 970-keV level was measured to be $\leq 7.7\times10^{-3}$ from

the γ-ray intensity balance experiment. Since this is a second-forbidden (mixed) transition, its EC/β^+ ratio and logft value were calculated as for an allowed transition. The resulting values are $\leq 1.2\times10^{-5}$ for the β^+ branching ratio and ≥ 7.4 for the logft value.

(iv) The most stringent limit on the branching ratio for the isospin forbidden Fermi EC transition to the 1451-keV level was determined to be $\leq 5.0\times10^{-3}$ from the γ-ray intensity balance experiment. From this limit and the formulae in Ref. 7, we derive an upper limit of 124 keV for the strength of the isospin mixing Coulomb matrix element between the $T=0$ ground and the $T=1$ analog state of ^{56}Ni. This contrasts with the largest observed values of 56 keV for ^{57}Ni and 41.7 keV for ^{64}Ga. Unfortunately, a theoretical estimate for isospin mixing in ^{56}Ni is not presently available.

Theoretically, the fastest β^+ transition of ^{56}Ni is expected to be that to the 158-keV level. Our experimental limit of 2.9×10^4 years for the partial β^+ half-life of ^{56}Ni is a factor of approximately 3 lower than the smallest theoretical estimate. However, since our solar system is about 30 000 light years from the center of the galaxy, this result already implies that highly relativistic ^{56}Ni produced over a large volume of the galaxy would be able to survive in the cosmic rays and reach the earth. The detection of ^{56}Ni in the cosmic rays would thus place a strong constraint on the acceleration mechanism for relativistic nuclei in the cosmic rays, or, if a model is assumed, its abundance could be used to determine the rate of supernova explosions in our galaxy. We therefore reiterate the need for further experimental effort in this direction.

ACKNOWLEDGMENTS

We would like to thank R. B. Firestone for supplying some of the computer programs used in this work, and R. G. Helmer for useful discussions and calculations. We also wish to thank M. M. Hindi for his assistance in deriving the formulas used for analyzing the data from the anticoincidence experiment. This work was supported by the U.S. Department of Energy under Contract No. DE-AC03-76SF00098.

[1] C. M. Lederer and V. S. Shirley, *Table of Isotopes*, 7th Ed. (Wiley, New York, 1978).
[2] K. T. Lesko, E. B. Norman, B. Sur, and R.-M. Larimer, Phys. Rev. C **40**, 445 (1989).
[3] P. A. Pinto and S. E. Woosley, Nature **333**, 534 (1988).
[4] L. W. Wilson, Ph.D. thesis, University of California, 1978 (Lawrence Berkeley Laboratory Report No. LBL-7723, 1978).
[5] E. K. Warburton, G. T. Garvey, and I. S. Towner, Ann. Phys. (N.Y.) **57**, 174 (1970).
[6] M. Cassé, Proc. 13th Intl. Cosmic Ray Conf. **1**, 546 (1973).
[7] S. Raman, T. A. Walkiewicz, and H. Behrens, At. Data Nucl. Data Tables **16**, 451 (1975).
[8] S. Hofman, Z. Phys. **270**, 133 (1974).
[9] L. E. Samuelson *et al.*, Phys. Rev. C **7**, 2379 (1973).
[10] J. Piluso, D. O. Wells, and D. K. McDaniels, Nucl. Phys. **77**, 193 (1966).
[11] J. T. Routti and S. G. Prussin, Nucl. Instrum. Methods **72**, 125 (1969).
[12] B. Chauvenet, J. Morel, and J. Legrand, Int. J. Appl. Radiat. Isotop. **34**, 479 (1983).
[13] K. Debertin, Nucl. Instrum. Methods **158**, 479 (1979).
[14] Y. Yoshizawa, Y. Iwata, and Y. Iinuma, Nucl. Instrum. Methods **174**, 133 (1980).
[15] K. Debertin and R. G. Helmer, *Gamma- and X-Ray Spectrometry with Semiconductor Detectors* (North-Holland, Amsterdam, 1988).
[16] KORSUM, a computer code for calculating coincidence-summing corrections, K. Debertin, *Gamma- and X-Ray Spectrometry with Semiconductor Detectors*, Ref. 15, p. 263.
[17] R. G. Helmer (private communication).
[18] R. C. Jenkins and W. E. Meyerhof, Nucl. Phys. **58**, 417 (1964).
[19] H. Junde *et al.*, Nucl. Data Sheets **51**, 1 (1987).
[20] L. Lyons, *Statistics for Nuclear and Particle Physicists* (Cambridge University Press, Cambridge, 1986), p. 78.
[21] Particle Data Group, Phys. Lett. B **204**, 1 (1988).
[22] Zhou Chunmei *et al.*, Nucl. Data Sheets **48**, 111 (1968).
[23] W. J. Worthington, Jr., Phys. Rev. **87**, 158 (1952).
[24] S. Monaro, R. A. Ricci, and R. van Lieshout, Nuovo Cimento Suppl. **19**, 329 (1961).
[25] R. K. Sheline and R. W. Stoughton, Phys. Rev. **87**, 1 (1952).
[26] D. O. Wells, S. L. Blatt, and W. E. Meyerhof, Phys. Rev. **130**, 1961 (1963).